IEEE Photonics Journal
An IEEE Photonics Society Publication

Open Access

Analysis of Polarization-Dependent Light Extraction and Effect of Passivation Layer for 230-nm AlGaN Nanowire Light-Emitting Diodes

Volume 9, Number 4, August 2017

Yu Kee Ooi
Cheng Liu
Jing Zhang

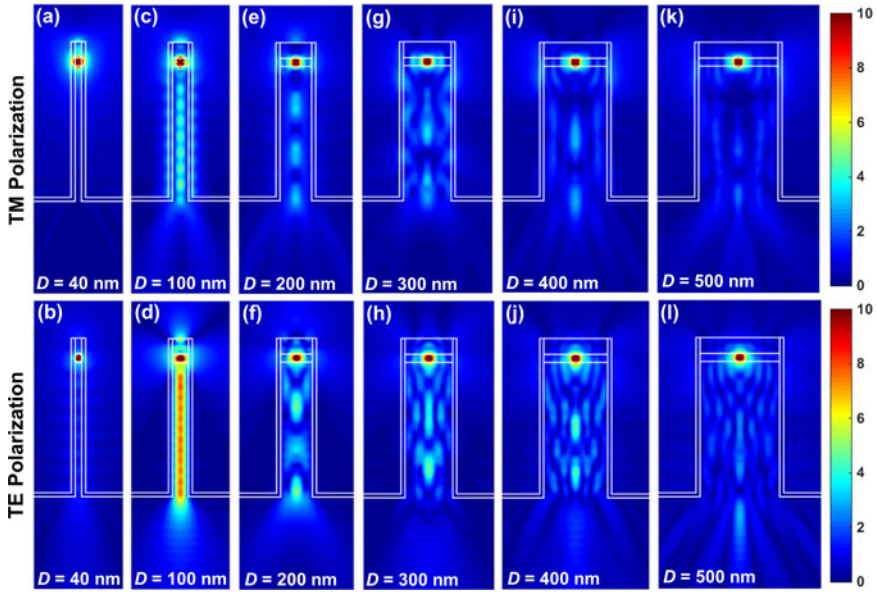

DOI: 10.1109/JPHOT.2017.2710325
1943-0655 © 2017 IEEE

IEEE photonics SOCIETY

IEEE

Analysis of Polarization-Dependent Light Extraction and Effect of Passivation Layer for 230-nm AlGaN Nanowire Light-Emitting Diodes

Yu Kee Ooi,[1] Cheng Liu,[1] and Jing Zhang[1,2]

[1]Microsystems Engineering, Rochester Institute of Technology, Rochester, NY 14623 USA
[2]Department of Electrical and Microelectronic Engineering, Rochester Institute of Technology, Rochester, NY 14623 USA

DOI:10.1109/JPHOT.2017.2710325

Manuscript received May 1, 2017; revised May 25, 2017; accepted May 27, 2017. Date of publication June 8, 2017; date of current version June 23, 2017. This work was supported in part by the Rochester Institute of Technology Kate Gleason endowed professorship fund and in part by the Office of Naval Research under Grant N00014-16-1-2524. Corresponding author: Yu Kee Ooi (e-mail: Yu.Kee.Ooi@rit.edu)

Abstract: This paper investigates the polarization-dependent light extraction efficiency ($\eta_{extraction}$) and the effect of passivation layer for AlGaN-based nanowire (NW) deep-ultraviolet (DUV) light-emitting diodes (LEDs) emitted at 230 nm using three-dimensional finite-difference time-domain method. Our results show that the use of NW structure for 230-nm LEDs can result in higher transverse-magnetic (TM) polarized $\eta_{extraction}$ than transverse-electric (TE) polarized $\eta_{extraction}$. Specifically, $\eta_{extraction}$ up to ~48% for TM polarization and ~41% for TE polarization can be achieved by the investigated 230-nm NW LEDs as compared to conventional planar LEDs (~0.2% and ~2% for TM- and TE-polarizations, respectively) attributed to the large surface-to-volume ratio and strong sidewall emissions. In addition, the analysis on the effect of various passivation layer materials suggests the use of SiO_2, which has smaller refractive index than the NW core, could extract more photons out of the NW core and lead to TM-polarized $\eta_{extraction}$ up to ~47%. Therefore, the use of the AlGaN NW structure is expected to lead to high external quantum efficiency DUV LEDs due to the large TM-polarized $\eta_{extraction}$ in combination with the dominant TM-polarized spontaneous emissions at 230 nm.

Index Terms: Light-emitting diodes, ultraviolet, finite-difference time-domain method, nanowire, polarization-dependent light extraction efficiency, AlGaN quantum well.

1. Introduction

III-Nitride based semiconductor ultraviolet (UV) emitters have great potential in replacing bulky mercury lamps and excimer lasers attributing to their compact size, lower operating voltage, excellent tunability, higher energy efficiency and longer lifetime. As a result, AlGaN-based UV light-emitting diodes (LEDs) and laser diodes have attracted significant attention recently as new UV light sources for various applications such as semiconductor photolithography, resin curing for 3D printing, water and air purification, sterilization, bioagent detection, and biological and chemical sensing [1]–[4]. In spite of these many advantages, the efficiency of AlGaN-based UV LEDs, especially for deep-UV (DUV) LEDs with emission wavelength (λ) $<$ 250 nm, is still extremely low compared to its visible

counterparts that are based on InGaN active regions. The external quantum efficiency (η_{EQE}) of AlGaN quantum well (QW) UV LEDs with planar structure has been reported to be less than 10% for $\lambda < 300$ nm, and further drops to $\sim$1% when λ is below 250 nm [3], [5]. Several factors have been identified to contribute to this extremely low UV LED efficiency: 1) difficulties in p-type doping of AlGaN layer, 2) challenges in making good ohmic contact on high Al-content AlGaN layer, 3) large dislocation density from AlGaN materials, and 4) the valence subbands crossover [6]–[11] at high Al-composition AlGaN QW active region that results in dominant transverse-magnetic (TM) [$\boldsymbol{E}$ //c-axis] polarized output in DUV regime. Subsequently, extensive works have been focused on thin film growth techniques and surface patterning to address issues associated with the low η_{EQE} in high Al-composition AlGaN-based UV LEDs [12]–[23]. Quantitative analysis on various LED structures such as micro-dome design [24], patterned sapphire substrate [25], and flip chip design [26], [27] to improve the UV LED light extraction efficiency ($\eta_{extraction}$) have also been carried out. Despite these continuous efforts, it remains extremely challenging to realize high-efficiency AlGaN-based UV LEDs with planar structure.

On the contrary, recent studies on AlGaN-based nanowire (NW) structure have reported encouraging device performance for mid- and DUV LEDs [28]–[30]. Experimental studies on NW UV LEDs have demonstrated substantial improvement in the internal quantum efficiency (η_{IQE}) for peak emission wavelength (λ_{peak}) of 340 nm [28] down to 210 nm [30] attributed to dislocation-free materials and improved p-type doping. Another key advantage by the use of NW design is the enhancement of $\eta_{extraction}$ due to the significantly improved surface-to-volume ratios [28]–[31]. NW design with larger surface area than conventional planar structure can allow more light to escape through the sidewall, which in turn will lead to larger $\eta_{extraction}$. While experimental studies have demonstrated promising results for UV LEDs with NW structures, there has been very limited work devoted to investigating the polarization-dependent $\eta_{extraction}$ for AlGaN-based NW UV LEDs which is of great importance due to the existence of the valence subbands crossover [6], [7] that results in TM-dominant spontaneous emission in the DUV regime.

Note that previous works [31], [32] have theoretically investigated the light extraction properties of the 280 nm AlGaN NW LEDs and concluded dominant TM-polarized light extraction from those structures. However, due to the significantly low TM-polarized spontaneous emission rate (R_{sp}) at 280 nm [6], [7], it is still very difficult to achieve a promising η_{EQE}. On the other hand, it is important to note that the TM$-R_{sp}$ will become dominant for wavelengths at 230 nm as the crystal-field split-off (CH) subband occupies the highest energy level in conventional AlGaN-based active region with high Al-compositions [6], [7]. Nevertheless, the polarization-dependent light extraction mechanism has not been studied yet for this DUV regime.

Therefore, in this study, we examined the transverse-electric (TE)- [$\boldsymbol{E} \perp$ c-axis] and TM-polarized $\eta_{extraction}$ of AlGaN-based NW DUV LEDs based on finite-difference time-domain (FDTD) method, which has been widely used in optical property analysis of III-Nitride emitters [24], [26], [27]. In particular, we investigated the light extraction properties of 230 nm NW LEDs with various NW sizes and passivation layer materials, and have conducted comparison study with conventional planar AlGaN QW DUV LEDs.

2. 3D FDTD Simulation Method

In this study, three-dimensional (3D) FDTD method [33] is used to analyze the $\eta_{extraction}$ and field distributions for AlGaN-based NW DUV LEDs at 230 nm. The 3D FDTD calculation is a commonly used technique in studying the propagation of photons in response to a given electromagnetic excitation by solving the Maxwell's curls equations with specific boundary conditions based on Yee's mesh. During the simulation, the electric field ($\boldsymbol{E}_x$, $\boldsymbol{E}_y$ and $\boldsymbol{E}_z$) and magnetic field ($\boldsymbol{H}_x$, $\boldsymbol{H}_y$ and $\boldsymbol{H}_z$) components, which are interlaced in Yee's mesh cell with grid points spaced Δx, Δy, and Δz apart, at a given mesh point, are solved discretely in time domain based on the set of differential form of Maxwell's equations. Comprehensive discussion on FDTD method can be found in [34].

The layer structure of the simulated NW UV LED investigated in this study, as depicted in Fig. 1(a), consists of a 200-nm thick sapphire substrate, a 1.5-μm thick n-AlN, a 50-nm thick AlGaN

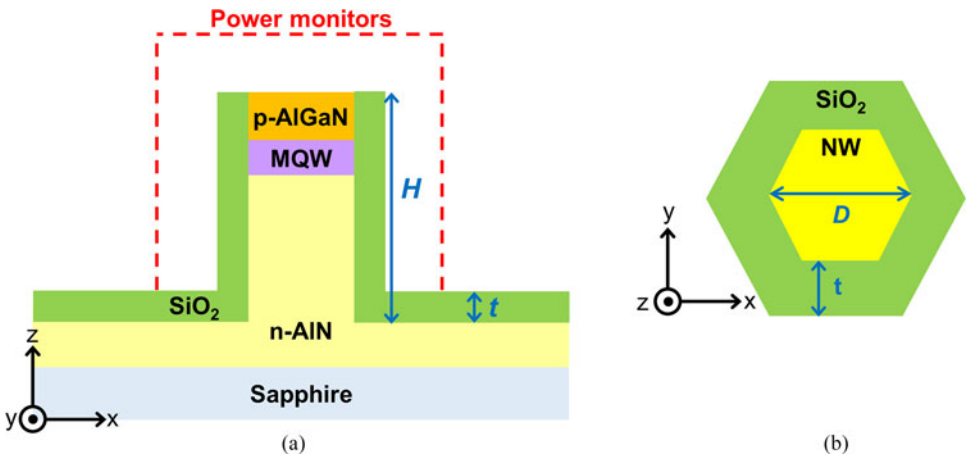

Fig. 1. (a) Schematic of AlGaN-based NW UV LED with SiO_2 passivation layer, (b) cross-sectional view of NW from top.

layer to represent the multiple quantum wells (MQWs) active region, a 100-nm thick p-AlGaN layer, and a 25-nm thick SiO_2 passivation layer. The NW consists of a hexagonal shape MQW core of diameter *D* and height *H* surrounded by a 25-nm thick SiO_2 shell layer [Fig. 1(b)], and is oriented along the c-axis, which is parallel to the z-direction labeled in Fig. 1. The refractive indexes for sapphire, AlN, AlGaN, and SiO_2 layers are set as 1.9, 2.3, 2.4 and 1.52 respectively [35] while the absorption coefficients of the n-AlN, AlGaN active region and p-AlGaN are assumed to be 10 cm^{-1}, 1000 cm^{-1} and 11500 cm^{-1} respectively [32], [35]. The simulation domain is set to $\sim 2\lambda + D$ with non-uniform grid size (5 nm in the bulk and 2.5 nm at the edge). Perfectly matched layer (PML) boundary condition is applied to all the boundaries to absorb all outgoing waves incident upon it.

A single dipole source with $\lambda = 230$ nm is placed at the center of the AlGaN MQW active region where TE-polarization is defined as the major electric field travels in the in-plane direction [$\boldsymbol{E} \perp$ c-axis] while TM-polarization is represented by the major electric field travels in the out-of-plane direction [$\boldsymbol{E}$ // c-axis]. Single dipole source has been used in this work as previous study has pointed out that the use of multiple dipole sources will result in non-physical interference pattern [36], which is undesirable for analysis of the optical properties of LEDs. A source power monitor surrounding the dipole source is used to measure the total power generated in the active region while output power monitors are placed at distance λ away from the NW to measure the light output power radiated out of the LED device. One field monitor is positioned at the center of the NW x-z plane to track the near-field electric field distribution along the NW. The $\eta_{extraction}$ is calculated as the ratio of the light output power measured by the output power monitors to the total emitted power in the active region measured by the source power monitor [32]. Note that a single AlGaN-based NW structure is used here for analysis, which is commonly employed in the study of the optical properties of NW structure LEDs in both experimental and theoretical works [32], [37]–[40].

A planar UV LED with similar layer structure and thickness as the investigated NW UV LED depicted in Fig. 1 has been investigated for comparison purposes. Due to the limitation of computation resources, the lateral simulation domain is set to 4 μm $\times$ 4 μm [26] with non-uniform grid size of 5 nm in the bulk and 2.5 nm at the edge. The refractive indexes and absorption coefficients for AlN and sapphire layers are taken from [35] while for GaN layer is taken from [41]. Linear extrapolation between AlN and GaN is used in calculating the refractive indexes and absorption coefficients for p-AlGaN layer and AlGaN active region, where the Al-content for the corresponding emission wavelength is determined from [23]. In addition, a single output power detection plane located at distance λ away from the top of p-type layer is used to measure the light output power radiated out of the planar LED device [26].

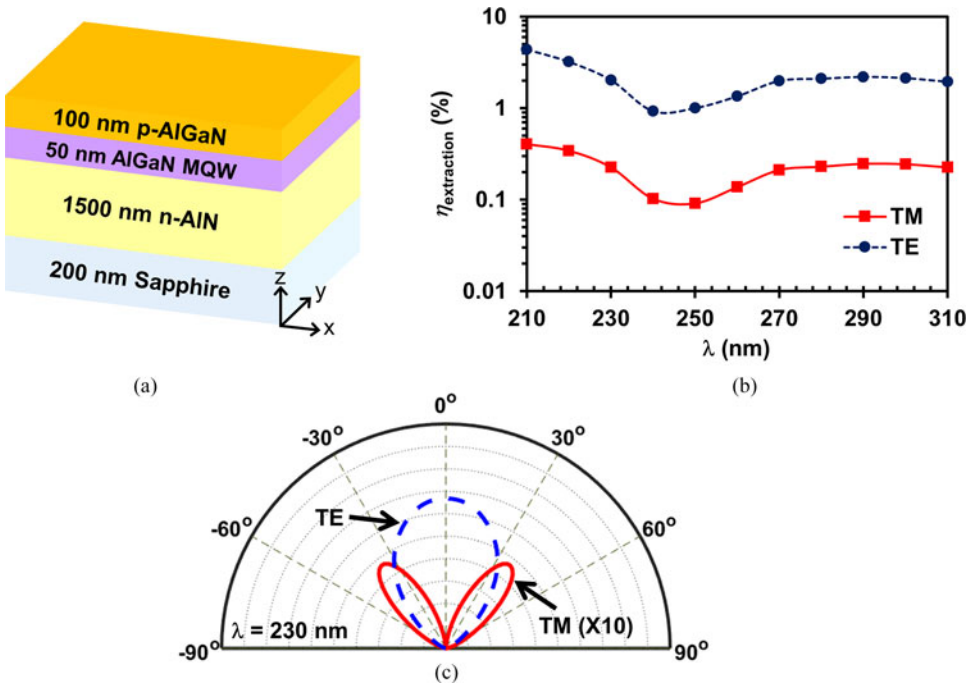

Fig. 2. (a) Schematic of planar structure UV LED, (b) $\eta_{extraction}$ of the planar UV LEDs as a function of λ, (c) polar plot of far-field intensities of planar UV LEDs for $\lambda = 230$ nm.

3. Results and Discussion

3.1 Planar UV LED Structure as a Comparison

Planar structure UV LEDs for λ ranges from 210 nm to 310 nm have been investigated for comparison purpose. Fig. 2(a) illustrates the schematic of the planar structure AlGaN-based MQW UV LED with the corresponding layers thicknesses. The $\eta_{extraction}$ for each polarization as a function of λ is presented in Fig. 2(b). The result shows that the planar LED always has higher TE-polarized $\eta_{extraction}$ ($\sim$1 – 4%) than TM-polarized $\eta_{extraction}$ ($\sim$0.1 – 0.4%) as λ changes from 210 to 310 nm, which is consistent with the result reported in previous analytical study for AlGaN-based UV LED emits at 280 nm ($\sim$4% for TE polarization and $\sim$0.4% for TM polarization) [32]. As planar structure favors light extraction from the top/bottom surface (along c-axis) while TM-polarized light tends to emit at large angles with respect to c-axis, as evidenced by polar plot of the far-field intensities in Fig. 2(c), majority of TM-polarized output will be trapped inside the planar structure due to total internal reflection and eventually being re-absorbed by the LED device. As a result, smaller TM-polarized $\eta_{extraction}$ ($\sim$0.1 – 0.4%) is obtained, which is approximately one order of magnitude lower than the TE-polarized $\eta_{extraction}$ ($\sim$1 – 4%).

Despite the fact that the TE-polarized $\eta_{extraction}$ for AlGaN MQW planar LED is significantly higher than the TM-polarized $\eta_{extraction}$ for $\lambda \sim$ 210–310 nm, it is very challenging to achieve large TE-R_{sp} for such wavelength regime (as shown in Fig. 3). The spontaneous emission spectra of AlGaN/AlN QW with Al-content ranging from 50% to 80% at carrier density (n) of 5×10^{18} cm^{-3} presented in Fig. 3 were calculated based on the 6-band $\boldsymbol{k \cdot p}$ formalism and taking into account strain effect, valence band mixing, spontaneous and piezoelectric polarization, as well as the carrier screening effect [6], [10]. Due to the valence subbands crossover from the AlGaN QWs, only significantly large TM-polarized R_{sp} can be obtained at $\sim$230 nm due to the dominant conduction band to CH subband transition (C-CH). However, even with this large TM$-R_{sp}$ at 230 nm, it is still extremely challenging to realize high-efficiency planar 230 nm LEDs due to the extremely low TM-polarized $\eta_{extraction}$ ($\sim$0.2%) [Fig. 2(b)]. Consequently, it provides a strong motivation to investigate the polarization-dependent

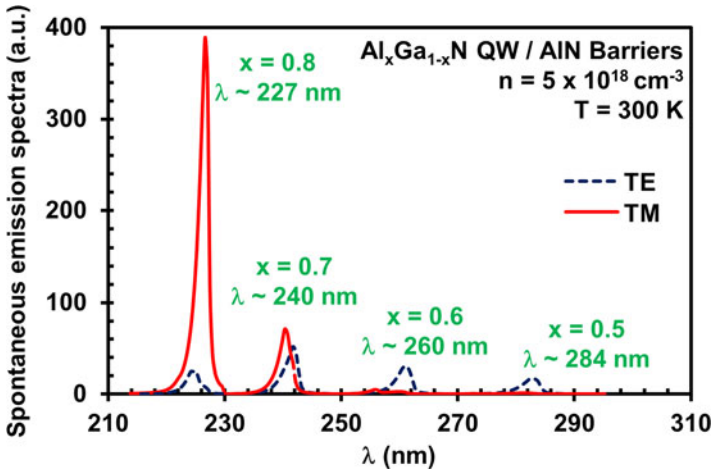

Fig. 3. Spontaneous emission spectra for $Al_xGa_{1-x}N$ QW with various Al-composition plotted as a function of its corresponding emission wavelength at room temperature with carrier density, n = 5 x 10^{18} cm^{-3}.

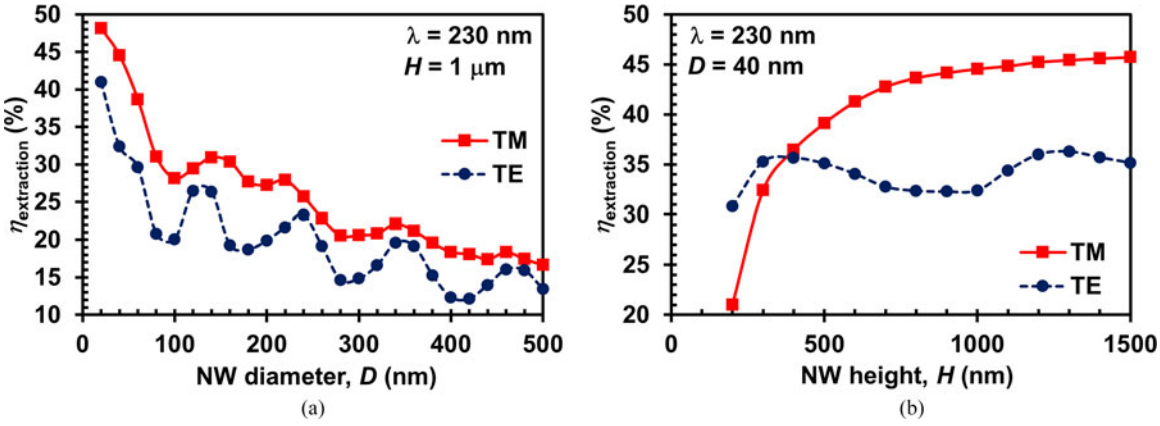

Fig. 4. The $\eta_{extraction}$ of the investigated NW UV LEDs as a function of (a) NW diameter (D) ranges from 20 nm to 500 nm with NW height, $H = 1$ μm, and (b) NW H ranges from 200 nm to 1500 nm with NW $D = 40$ nm.

$\eta_{extraction}$ of AlGaN-based NW UV LEDs, especially in the 230 nm regime, if a strong TM-polarized $\eta_{extraction}$ can be obtained otherwise.

3.2 Nanowire UV LED Structures

The $\eta_{extraction}$ of the 230 nm NW LEDs for both TE- and TM-polarizations are examined here, and the results are presented in Fig. 4. Fig. 4(a) plots the $\eta_{extraction}$ as a function of NW diameter (D) ranging from 20 nm to 500 nm with NW height (H) of 1 μm. The result shows that NW structure favors TM-polarized emission, as the TM-polarized $\eta_{extraction}$ is consistently higher than the TE-polarized $\eta_{extraction}$ for the investigated NW D range. As an example, ~45% of $\eta_{extraction}$ can be achieved for TM-polarized emission while ~32% of $\eta_{extraction}$ is obtained for TE-polarized emission when $D =$ 40 nm, which corresponding to ~238 and ~17 times enhancement in the TM- and TE-polarized $\eta_{extraction}$ respectively as compared to the conventional planar structure. As D increases to 100 nm, the $\eta_{extraction}$ drops to ~28% for TM-polarization and ~20% for TE-polarization, but still the $\eta_{extraction}$ is ~149 times for TM-polarization and ~10 times for TE-polarization higher than the conventional

planar structure. In addition, the fluctuations in the $\eta_{extraction}$ for both TM- and TE-polarizations are due to the formation of resonant modes inside the NW core [32]. In contrast to the planar structure UV LEDs, NW structure with larger sidewall surface area is more efficient in extracting TM-polarized emission. As the dominant R_{sp} would be TM-polarized (Fig. 3) for the corresponding AlGaN QW employed in the NW LED active region, significantly improved η_{EQE} would be expected for the investigated NW UV LEDs as a result of the high TM-polarized $\eta_{extraction}$ and large TM-polarized R_{sp}. It is also interesting to point out that as D increases from 20 nm to 500 nm, the general trend of the $\eta_{extraction}$ for both TE- and TM-polarizations is gradually declined due to the slight decrease in the surface-to-volume ratio, which results in increased portion of light being trapped inside the LED NW structure.

Note that the effects of small NW D on the η_{IQE} is also an important consideration for the overall LED performance. Previous studies have shown that NW structure exhibits significantly reduced defect density, which in turn decreases the probability of non-radiative recombination at the defect sites. In addition, the reduced strain distribution in the NW structure induces smaller piezoelectric polarization field that results in negligible quantum confined Stark effect in the NW [28], [42]–[45]. Therefore, the use of NW structure which favors TM-polarized light extraction, in conjunction with improved η_{IQE}, it is expected that the overall efficiency can be boosted which makes it an ideal candidate for high-efficiency TM-polarized DUV emitter.

The dependence of the $\eta_{extraction}$ for both TE- and TM-polarizations for the investigated NW UV LEDs with various NW H is presented in Fig. 4(b). As H changes from 200 nm to 800 nm, the TM-polarized $\eta_{extraction}$ increases sharply from $\sim$21% to $\sim$44%, and levels off at $\sim$45% for $H >$ 800 nm. Conversely, the NW H has less effect on the TE-polarized $\eta_{extraction}$ where it primarily oscillates between $\sim$30% and $\sim$35% as the NW H changes from 200 nm to 1500 nm. The minimal changes in the $\eta_{extraction}$ for the TM-polarization emission when NW H varies from 800 nm to 1500 nm are due to the lateral propagation direction of TM-polarized photons that lead to strong photon extraction near the active region. Accordingly, longer NW H will not result in significant photon extraction along the NW sidewall that is further away from the active region. For the case of TE-polarization emission, since majority of the TE-polarized photons are traveling in vertical direction and being trapped inside the NW, only a small portion of TE-polarized photons can leak out through the NW sidewall. As a result, the formation of resonant modes inside the NW due to the severe photons trapping is causing the TE-polarized $\eta_{extraction}$ to fluctuate. Therefore, optimum NW H ranges between 800 nm and 1000 nm is preferable for the investigated NW UV LEDs when $D = 40$ nm.

In order to better understand the photon extraction by the use of NW structure, Fig. 5 shows the electric field intensity distribution for the investigated NW UV LEDs at x-z plane with various NW D. The NW H is fixed at 1 μm. For TM-polarized emission (top row figures of Fig. 5), majority of the light is travelling in lateral direction while very limited photons are propagating in vertical direction. As a result, TM-polarized light can easily escape through the NW sidewall, especially for NW structure with small D [Fig. 5(a)], which results in significantly improved TM-polarized $\eta_{extraction}$ ($\sim$45% for the case of $D = 40$ nm) as compared to conventional planar structure ($\sim$0.2%). In contrast, TE-polarized photons (bottom row figures of Fig. 5) are mainly propagating in vertical direction which can only be extracted out from the top and bottom sides of the NW while very limited photons are emitted in lateral direction to be extracted out through the NW sidewall. Due to the absorption by p-AlGaN layer and the undesired bottom emitting through sapphire substrate, lower TE-polarized $\eta_{extraction}$ is obtained as compared to the TM component [Fig. 4(a)]. Nevertheless, the $\eta_{extraction}$ for both TM- and TE-polarizations by the use NW structure is still larger than conventional planar structure. For NW structure which has large surface-to-volume ratio, photons can escape into the air medium much easier through the NW sidewall than conventional planar structure as photons in conventional planar structure can only be extracted out through the top and bottom surfaces. As the emission from 230 nm LED is strongly TM-polarized (Fig. 3), strong sidewall TM-polarized photons extraction by the use of NW structure is expected to improve the overall UV LED performance significantly.

The electric field intensity plots presented in Fig. 5 also provide insight into the impact of NW structural parameters to the $\eta_{extraction}$. For NW UV LED with $D = 40$ nm and $H = 1$ μm, majority

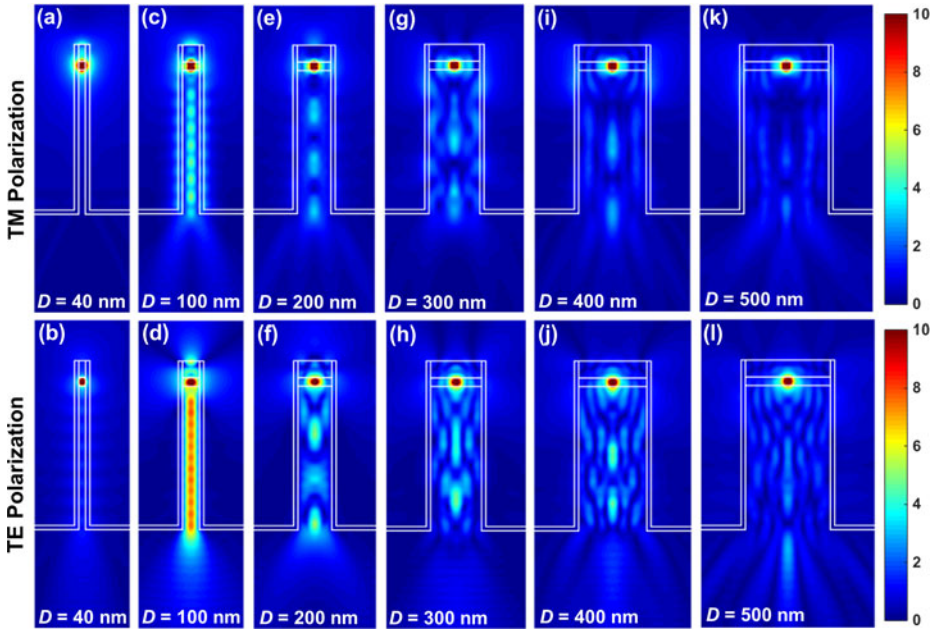

Fig. 5. Cross-sectional near-field electric field intensity of the investigated NW UV LEDs with $H = 1\ \mu$m and various D for TM-polarization (top row figures) and TE-polarization (bottom row figures) at x-z plane.

of TM-polarized photons are escaped through sidewall of the NW [Fig. 5(a)] while TE-polarized photons are generally trapped along the NW [Fig. 5(b)]. As D increases to 100 nm [Fig. 5(c) and (d)], the trapping of photons becomes more obvious for both TM- and TE-polarizations due to the weak micro-cavity effect. Nevertheless, significant amount of photons can still be extracted out through the NW sidewall for TM-polarized emission, even though the strong photons confinement inside the NW structure for both polarizations result in a lower $\eta_{\text{extraction}}$ ($\sim$28% and $\sim$20% for TM- and TE-polarizations respectively) as compared to the case of $D = 40$ nm ($\sim$45% and $\sim$32% for TM- and TE-polarizations respectively). Further increasing the NW D [Fig. 5(e)–(l)] will lead to more photons trapping inside the NW structure and less photons extraction. However, due to the increment of photon absorption by the larger p-layer area and weaker resonant effect in larger dimension NW, the electric field intensity along the NW is getting weaker as compared to the case of $D = 100$ nm. For that reason, the ideal NW DUV LED is recommended to avoid NW design that strongly confines TM-polarized photons as well as NW structure with large area of p-type doping layer, which is $D > 80$ nm for the investigated NW UV LED structures with $H = 1\ \mu$m, in order to achieve high efficiency DUV LEDs. While the NW D undeniably plays a vital role in the $\eta_{\text{extraction}}$, it is worth noting that longer NW H with extended n-AlN region does not contribute to significant photons extraction since most of the near-field electric field intensity is concentrated around the AlGaN MQW active region. As a result, the light extraction through the NW sidewall region that is further away from the active region is very limited, especially for the case of $D \geq 100$ nm [Fig. 5(c)–(l)]. Therefore, the $\eta_{\text{extraction}}$ remains nearly constant ($\sim$45% for TM-polarization and $\sim$30 – 35% for TE-polarization) even though the NW H increases from 800 nm to 1500 nm [Fig. 4(b)].

3.3 Effect of Passivation Layer on TM-Polarized $\eta_{\text{extraction}}$ for Nanowire UV LEDs

The large surface area for NW structure gives rise to the presence of high surface density states due to the non-radiative recombination near the surface, which in turn will lead to degraded quantum efficiency and lower output power for NW devices [46], [47]. Therefore, passivation layer for NW structure plays an important role in suppressing the surface recombination arising from the surface

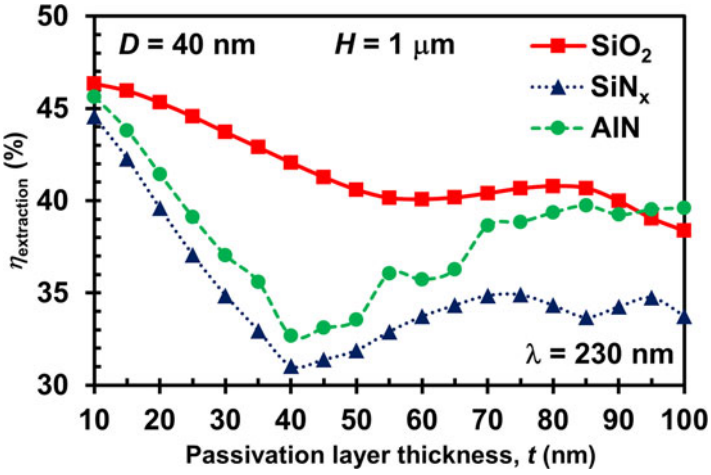

Fig. 6. The TM-polarized $\eta_{extraction}$ of the investigated NW UV LEDs with different passivation layer materials as a function of passivation layer thickness (t) with NW $H = 1\ \mu$m and $D = 40$ nm.

states. On the other hand, the choice of passivation layer material and its corresponding thickness are critical for $\eta_{extraction}$ as the passivation layer could possibly impede the light extraction if the design is not optimized. Ideally, it is preferred for the passivation layer to appear transparent in the LED emission range, and have smaller refractive index than the NW core structure to minimize the cavity effects that cause severe photons trapping within the NW core. This increases the possibility of photon extraction which in turn contributes to larger $\eta_{extraction}$.

In order to examine the effect of passivation layer on the TM-polarized $\eta_{extraction}$ for NW DUV LED, we study the NW UV LEDs with 3 different commonly used passivation layers for nitride-based LED – SiO_2, SiN_x and AlN. At $\lambda = 230$ nm, the refractive indexes of SiO_2, SiN_x and AlN are 1.52, 2.35 and 2.3 respectively [35]. SiO_2 layer appears transparent for the investigated wavelength regime ($\lambda = 230$ nm) with negligible absorption while SiN_x and undoped AlN layers are assumed to have absorption coefficient of 11000 cm^{-1} and 10 cm^{-1} respectively [32], [35]. The TM-polarized $\eta_{extraction}$ presented in Fig. 6 as a function of passivation layer thickness (t) ranges from 10 nm to 100 nm shows that NWs with SiO_2 passivation layer exhibit the highest $\eta_{extraction}$ than NWs with SiN_x or AlN passivation layer. The SiO_2 passivation layer with smaller refractive index ($n = 1.52$) than the NW core ($n = 2.4$) can prevent the existence of strong cavity effect inside the NW core that traps photons due to reduced total internal reflection. At the same time, SiO_2 also has the lowest absorption coefficient compared to SiN_x and AlN, which in turn will lead to more photon extraction that contributes to higher $\eta_{extraction}$. For SiN_x and AlN, even though the refractive indexes for these two materials are very similar, SiN_x has larger photon absorption than AlN. As a result, smaller $\eta_{extraction}$ are observed for NWs with SiN_x passivation layer.

Although both refractive index and absorption coefficient of passivation layer are critical to the $\eta_{extraction}$, varies passivation layer thicknesses will also affect the photon extraction through the NW sidewall. As shown in Fig. 6, NW UV LEDs with 40 nm NW D, 1 μm NW H and 10 nm thin passivation layer for all 3 different passivation layer materials exhibit very similar TM-polarized $\eta_{extraction}$ ($\sim$45 – 47%) as the properties of the extremely thin passivation layer only have minor effect on the photons. When t increases to 40 nm, which is similar to the NW D, the TM-polarized $\eta_{extraction}$ for NW with SiN_x and AlN passivation layer declines substantially to $\sim$31 – 33% due to total internal reflection and the coupling of resonant modes between the NW core and the passivation layer, while the TM-polarized $\eta_{extraction}$ for NW with SiO_2 passivation layer only decreases marginally to 42%. Further increasing the SiO_2 passivation layer thickness beyond 40 nm will result in even smaller TM-polarized $\eta_{extraction}$ ($\sim$38% with $t = 100$ nm) due to photons trapping inside the thick passivation layer that lead to larger coupling effects between the passivation layer and the NW core. However,

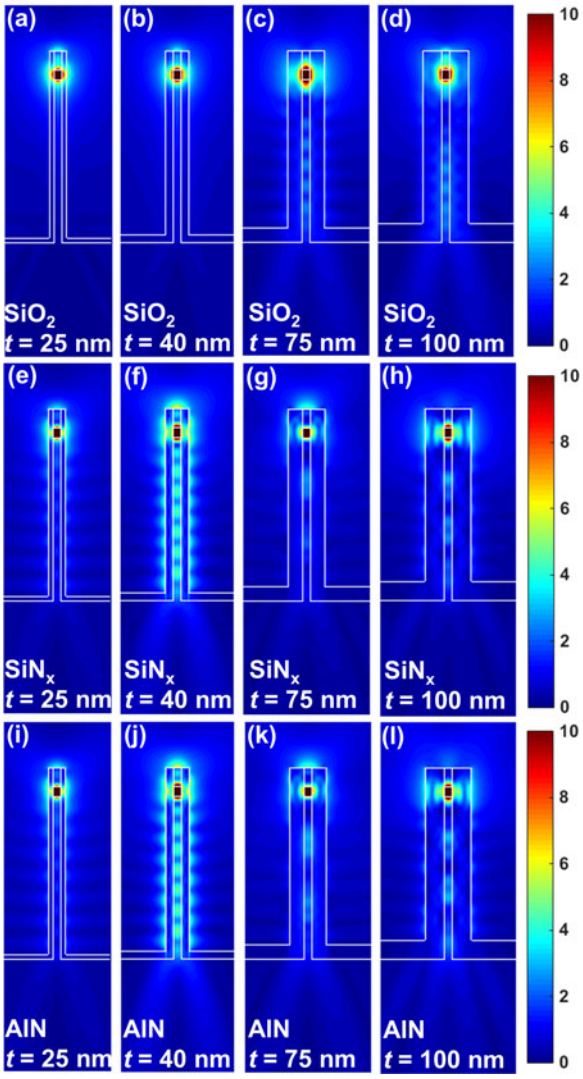

Fig. 7. Cross-sectional near-field electric field intensity of the investigated NW UV LEDs with various passivation layer materials for TM-polarization at x-z plane. The NW *D* and *H* are fixed at 40 nm and 1 μm respectively.

for the case of NW with SiN_x and AlN passivation layer, thicker passivation layer ($>$ 40 nm) is resulting in less severe photons trapping inside the NW core as the refractive indexes for SiN_x and AlN is very similar with the NW core. TM-polarized photons that travel laterally can easily move around the passivation layer and the NW core, which results in the formation of weak resonant modes in these two layers. Consequently, the weak coupling effects between resonant modes in the NW core and the passivation layer will lead to a gradual increase in the TM-polarized $\eta_{extraction}$. For example, $\eta_{extraction}$ of $\sim$35% and $\sim$39% are achieved for 75-nm thick SiN_x and AlN as passivation layer respectively. For NW with AlN passivation layer $t >$ 75 nm, the TM-polarized $\eta_{extraction}$ remains nearly constant, and is very similar to that of NW with SiO_2 passivation layer ($\sim$40% for both cases) attributed to the weaker resonant modes in the thick AlN passivation layer and subsequently smaller coupling effects. The TM-polarized $\eta_{extraction}$ for NW with SiN_x passivation layer stays below $\sim$35% as $t >$ 75 nm due to the large photon absorption by the SiN_x material.

To further understand the effect of various passivation layer designs to the TM-polarized $\eta_{extraction}$, the electric field intensity distribution of NW with 25 nm, 40 nm, 75 nm and 100 nm thick passivation layer for SiO_2, SiN_x and AlN materials are presented in Fig. 7. The NW H and D are fixed at 1 μm and 40 nm respectively. As clearly illustrated in the electric field intensity plots, for NW with thin SiO_2 passivation layer ($t \leq 40$ nm) [Fig. 7(a) and (b)], the TM-polarized photons, which are primarily concentrated near the active region, can easily penetrate through the thin passivation layer and result in large $\eta_{extraction}$ ($\sim$42 – 47%). Further increases the SiO_2 passivation layer thickness will result in some photons trapping along the NW core and the thick SiO_2 passivation layer [Fig. 7(c) and (d)]. Consequently, the coupling of light between the NW core and SiO_2 passivation layer is resulting in marginal reduction in the TM-polarized $\eta_{extraction}$ to $\sim$38% when $t = 100$ nm. For the case of 25 nm and 40 nm thin SiN_x or AlN passivation layers [Fig. 7(e), (f), (i), and (j)], majority of the TM-polarized photons suffer from total internal reflection which result in severe photons trapping along the NW core. As a result, the TM-polarized $\eta_{extraction}$ drops significantly from $\sim$45 – 46% with $t = 10$ nm to $\sim$31 – 33% with $t = 40$ nm. As t increases beyond 40 nm [Fig. 7(g), (h), (k), and (l)], despite the formation of resonant modes inside the thick passivation layer, the photons trapping along the NW core is less severe than the case of $t = 40$ nm. Subsequently, it leads to an upsurge in the TM-polarized $\eta_{extraction}$, $\sim$34% and $\sim$40% for NW with 100 nm thick SiN_x and AlN passivation layer respectively.

Therefore, in order to counterbalance the benefit of passivation layer in suppressing high surface density states and the negative impact of passivation layer on the $\eta_{extraction}$, SiO_2 and AlN are the preferred choices over SiN_x as the passivation layer materials for the investigated DUV NW LEDs. In particular, varying the thickness of SiO_2 passivation layer only has minimal impact on the TM-polarized $\eta_{extraction}$, which make it an ideal candidate as NW passivation layer. Nevertheless, considering the needs of a much straightforward fabrication step, AlN is in favor over SiO_2 as the former material can be grown in the same growth chamber as the NW core. It is recommended for NW with AlN passivation layer to have different passivation layer thickness than the NW D to minimize the strong coupling of resonant modes between the NW core and the passivation layer. In addition, previous experimental studies on nitride-based NW with AlGaN shell structure has reported that the use of rich Al-content AlGaN shell layer can effectively suppress the non-radiative recombination [28], [48], which can lead to improved η_{IQE}. Accordingly, thick AlN (> 75 nm) is expected to achieve high η_{EQE} for NW UV LEDs with AlN as passivation layer.

4. Conclusion

The TE- and TM-polarized $\eta_{extraction}$ of AlGaN-based NW LEDs emit at 230 nm with various NW structural parameters and passivation layers have been investigated intensively. Our analysis shows that TM-polarized $\eta_{extraction}$ up to $\sim$48% and TE-polarized $\eta_{extraction}$ up to $\sim$41% can be achieved with NW structure of various NW D and H as compared to conventional planar structure ($\sim$0.2% for TM-polarization and $\sim$2% for TE-polarization). Smaller NW D (< 60 nm) enables more photons to leak out through the NW sidewall that result in higher $\eta_{extraction}$ while increases the NW H beyond 800 nm has less impact on the $\eta_{extraction}$. In addition, the choice of passivation layer material and its corresponding thickness are also critical to the $\eta_{extraction}$. The use of SiO_2 as passivation layer which has smaller refractive index than the NW core can result in larger $\eta_{extraction}$ as compared to SiN_x and AlN. While varying the SiO_2 passivation layer thickness has minimal impact on the $\eta_{extraction}$, the thicknesses of SiN_x and AlN passivation layers are affecting the $\eta_{extraction}$ substantially. In summary, the investigated 230 nm NW LEDs with NW $D < 60$ nm, NW H ranges between 800 nm and 1000 nm, and thick SiO_2 or AlN (> 75 nm) passivation layer are anticipated to improve the η_{EQE} significantly attributed to the high TM-polarized $\eta_{extraction}$ and large TM-polarized R_{sp}, which are expected to be promising solutions to high-efficiency TM-polarized DUV emitters. Future work to address the impact of various NW design within an array of NW such as uniformity in NW diameter, height, spacing and peak emission wavelength as well as QW position is desired in order to provide a more comprehensive modeling of the NW LED performance.

References

[1] Y. Muramoto, M. Kimura, and S. Nouda, "Development and future of ultraviolet light-emitting diodes: UV-LED will replace the UV lamp," *Semicond. Sci. Technol.*, vol. 29, no. 8, Jun. 2014, Art. no. 084004.

[2] H. Hirayama, N. Maeda, S. Fujikawa, S. Toyoda, and N. Kamata, "Recent progress and future prospects of AlGaN-based high-efficiency deep-ultraviolet light-emitting diodes," *Jpn. J. Appl. Phys.*, vol. 53, no. 10, 2014, Art. no. 100209.

[3] M. Kneissl *et al.*, "Advances in group III-nitride-based deep UV light-emitting diode technology," *Semicond. Sci. Technol.*, vol. 26, no. 1, Jan. 2011, Art. no. 014036.

[4] M. Asif Khan, "AlGaN multiple quantum well based deep UV LEDs and their applications," *Phys. Status Solidi*, vol. 203, no. 7, pp. 1764–1770, May 2006.

[5] Y. Liao, C. Thomidis, C. Kao, and T. D. Moustakas, "AlGaN based deep ultraviolet light emitting diodes with high internal quantum efficiency grown by molecular beam epitaxy," *Appl. Phys. Lett.*, vol. 98, no. 2011, 2011, Art. no. 081110.

[6] J. Zhang, H. Zhao, and N. Tansu, "Effect of crystal-field split-off hole and heavy-hole bands crossover on gain characteristics of high Al-content AlGaN quantum well lasers," *Appl. Phys. Lett.*, vol. 97, no. 11, 2010, Art. no. 111105.

[7] J. E. Northrup *et al.*, "Effect of strain and barrier composition on the polarization of light emission from AlGaN/AlN quantum wells," *Appl. Phys. Lett.*, vol. 100, no. 2, 2012, Art. no. 021101.

[8] Y. Chang, F. Chen, S. Li, Y. Kuo, and M. Q. W. U. V Leds, "Electrical polarization effects on the optical polarization properties of AlGaN ultraviolet light-emitting diodes," *IEEE Trans. Electron Devices*, vol. 61, no. 9, pp. 3233–3238, Sep. 2014.

[9] Z. Bryan, I. Bryan, S. Mita, J. Tweedie, Z. Sitar, and R. Collazo, "Strain dependence on polarization properties of AlGaN and AlGaN-based ultraviolet lasers grown on AlN substrates," *Appl. Phys. Lett.*, vol. 106, no. 23, 2015, Art. no. 232101.

[10] C. Liu, Y. K. Ooi, and J. Zhang, "Proposal and physics of AlInN-delta-GaN quantum well ultraviolet lasers," *J. Appl. Phys.*, vol. 119, no. 8, 2016, Art. no. 083102.

[11] C. Liu *et al.*, "Physics and polarization characteristics of 298 nm AlN-delta-GaN quantum well ultraviolet light-emitting diodes," *Appl. Phys. Lett.*, vol. 110, no. 7, Feb. 2017, Art. no. 071103.

[12] C. Pernot *et al.*, "Improved efficiency of 255–280 nm AlGaN-based light-emitting diodes," *Appl. Phys. Exp.*, vol. 3, no. 6, Jun. 2010, Art. no. 061004.

[13] M. Akiba, H. Hirayama, Y. Tomita, Y. Tsukada, N. Maeda, and N. Kamata, "Growth of flat p-GaN contact layer by pulse flow method for high light-extraction AlGaN deep-UV LEDs with Al-based electrode," *Phys. Status Solidi Curr. Topics Solid State Phys.*, vol. 9, no. 3/4, pp. 806–809, 2012.

[14] T. Kinoshita *et al.*, "Performance and reliability of deep-ultraviolet light-emitting diodes fabricated on AlN substrates prepared by hydride vapor phase epitaxy," *Appl. Phys. Exp.*, vol. 6, no. 9, 2013, Art. no. 092103.

[15] P. Dong *et al.*, "282-nm AlGaN-based deep ultraviolet light-emitting diodes with improved performance on nano-patterned sapphire substrates," *Appl. Phys. Lett.*, vol. 102, no. 24, Jun. 2013, Art. no. 241113.

[16] N. Maeda and H. Hirayama, "Realization of high-efficiency deep-UV LEDs using transparent p-AlGaN contact layer," *Phys. Status Solidi Curr. Topics Solid State Phys.*, vol. 10, no. 11, pp. 1521–1524, 2013.

[17] J. J. Wierer, A. A. Allerman, I. Montaño, and M. W. Moseley, "Influence of optical polarization on the improvement of light extraction efficiency from reflective scattering structures in AlGaN ultraviolet light-emitting diodes," *Appl. Phys. Lett.*, vol. 105, no. 6, Aug. 2014, Art. no. 061106.

[18] S. Islam, V. Protasenko, S. Rouvimov, H. G. Xing, and D. Jena, "Sub-230 nm deep-UV emission from GaN quantum disks in AlN grown by a modified Stranski–Krastanov mode," *Jpn. J. Appl. Phys.*, vol. 55, no. 5S, May 2016, Art. no. 05FF06.

[19] E. Francesco Pecora *et al.*, "Sub-250 nm light emission and optical gain in AlGaN materials," *J. Appl. Phys.*, vol. 113, no. 1, 2013, Art. no. 013106.

[20] D. Y. Kim *et al.*, "Overcoming the fundamental light-extraction efficiency limitations of deep ultraviolet light-emitting diodes by utilizing transverse-magnetic-dominant emission," *Light Sci. Appl.*, vol. 4, no. 4, p. e263, Apr. 2015.

[21] H. Hirayama, N. Noguchi, and N. Kamata, "222 nm deep-ultraviolet AlGaN quantum well light-emitting diode with vertical emission properties," *Appl. Phys. Exp.*, vol. 3, no. 3, Mar. 2010, Art. no. 032102.

[22] M. Khizar, Z. Y. Fan, K. H. Kim, J. Y. Lin, and H. X. Jiang, "Nitride deep-ultraviolet light-emitting diodes with microlens array," *Appl. Phys. Lett.*, vol. 86, no. 17, pp. 1–3, 2005.

[23] H. Hirayama *et al.*, "222-282 nm AlGaN and InAlGaN-based deep-UV LEDs fabricated on high-quality AlN on sapphire," *Phys. Status Solidi*, vol. 206, no. 6, pp. 1176–1182, Jun. 2009.

[24] P. Zhao, L. Han, M. R. McGoogan, and H. Zhao, "Analysis of TM mode light extraction efficiency enhancement for deep ultraviolet AlGaN quantum wells light-emitting diodes with III-nitride micro-domes," *Opt. Mater. Exp.*, vol. 2, no. 10, pp. 1397–1406, 2012.

[25] X. Chen, C. Ji, Y. Xiang, X. Kang, B. Shen, and T. Yu, "Angular distribution of polarized light and its effect on light extraction efficiency in AlGaN deep-ultraviolet light-emitting diodes," *Opt. Exp.*, vol. 24, no. 10, pp. A935–A942, 2016.

[26] H.-Y. Ryu, I.-G. Choi, H.-S. Choi, and J.-I. Shim, "Investigation of light extraction efficiency in AlGaN deep-ultraviolet light-emitting diodes," *Appl. Phys. Exp.*, vol. 6, no. 6, Jun. 2013, Art. no. 062101.

[27] K. H. Lee *et al.*, "Light-extraction efficiency control in AlGaN-based deep-ultraviolet flip-chip light-emitting diodes: a comparison to InGaN-based visible flip-chip light-emitting diodes," *Opt. Exp.*, vol. 23, no. 16, pp. 20340–20349, 2015.

[28] Q. Wang *et al.*, "Highly efficient, spectrally pure 340 nm ultraviolet emission from $Al_xGa_{1-x}N$ nanowire based light emitting diodes," *Nanotechnology*, vol. 24, no. 34, Aug. 2013, Art. no. 345201.

[29] T. F. Kent, S. D. Carnevale, A. T. M. Sarwar, P. J. Phillips, R. F. Klie, and R. C. Myers, "Deep ultraviolet emitting polarization induced nanowire light emitting diodes with $Al_xGa_{1-x}N$ active regions," *Nanotechnology*, vol. 25, no. 45, 2014, Art. no. 455201.

[30] S. Zhao *et al.*, "Aluminum nitride nanowire light emitting diodes: Breaking the fundamental bottleneck of deep ultraviolet light sources," *Sci. Rep.*, vol. 5, Feb. 2015, Art. no. 8332.

[31] M. Djavid and Z. Mi, "Enhancing the light extraction efficiency of AlGaN deep ultraviolet light emitting diodes by using nanowire structures," *Appl. Phys. Lett.*, vol. 108, no. 5, 2016, Art. no. 051102.
[32] H.-Y. Ryu, "Large enhancement of light extraction efficiency in AlGaN-based nanorod ultraviolet light-emitting diode structures," *Nanoscale Res. Lett.*, vol. 9, no. 1, p. 58, 2014.
[33] FullWAVE, Synopsys's Optical Solutions Group. [Online]. Available: https://optics.synopsys.com
[34] A. Taflove and S. C. Hagness, *Computational Electrodynamics: The Finite-Difference Time-Domain Method*. Norwood, MA, USA: Artech House, 2005.
[35] E. D. Palik, *Handbook of optical constants of solids*. New York, NY, USA: Academic Press, 1998.
[36] P. Zhu, "Frustrated total internal reflection in organic light-emitting diodes employing sphere cavity embedded in polystyrene," *J. Opt.*, vol. 18, no. 2, Feb. 2016, Art. no. 025403.
[37] A.-L. Henneghien, B. Gayral, Y. Désières, and J.-M. Gérard, "Simulation of waveguiding and emitting properties of semiconductor nanowires with hexagonal or circular sections," *J. Opt. Soc. Amer. B*, vol. 26, no. 12, pp. 2396–2403, Dec. 2009.
[38] J. Chesin, X. Zhou, and S. Gradečak, "Light extraction in individual GaN nanowires on Si for LEDs," *Proc. SPIE*, vol. 8467, 2012, Art. no. 846703.
[39] M. Nami and D. Feezell, "Optical properties of Ag-coated GaN/InGaN axial and core–shell nanowire light-emitting diodes," *J. Opt.*, vol. 17, no. 2, Feb. 2015, Art. no. 025004.
[40] X. Zhou, M.-Y. Lu, Y.-J. Lu, E. J. Jones, S. Gwo, and S. Gradec˘ak, "Nanoscale optical properties of indium gallium nitride/gallium nitride nanodisk-in-rod heterostructures," *ACS Nano*, vol. 9, no. 3, pp. 2868–2875, 2015.
[41] C. H. Yan, H. Yao, J. M. Van Hove, a M. Wowchak, P. P. Chow, and J. M. Zavada, "Ordinary optical dielectric functions of anisotropic hexagonal GaN film determined by variable angle spectroscopic ellipsometry," *J. Appl. Phys.*, vol. 88, no. 6, pp. 3463–3469, Sep. 2000.
[42] W. Guo, M. Zhang, A. Banerjee, and P. Bhattacharya, "Catalyst-free InGaN/GaN nanowire light emitting diodes grown on (001) silicon by molecular beam epitaxy," *Nano Lett.*, vol. 10, no. 9, pp. 3356–3359, 2010.
[43] W. Guo, M. Zhang, P. Bhattacharya, and J. Heo, "Auger recombination in III-nitride nanowires and its effect on nanowire light-emitting diode characteristics," *Nano Lett.*, vol. 11, no. 4, pp. 1434–1438, 2011.
[44] Q. Wang, J. Bai, Y. P. Gong, and T. Wang, "Influence of strain relaxation on the optical properties of InGaN/GaN multiple quantum well nanorods," *J. Phys. D. Appl. Phys.*, vol. 44, no. 39, 2011, Art. no. 395102.
[45] G. Jacopin *et al.*, "Photoluminescence polarization in strained GaN/AlGaN core/shell nanowires," *Nanotechnology*, vol. 23, no. 32, 2012, Art. no. 325701.
[46] A. Armstrong, Q. Li, Y. Lin, A. A. Talin, and G. T. Wang, "GaN nanowire surface state observed using deep level optical spectroscopy," *Appl. Phys. Lett.*, vol. 96, no. 16, Apr. 2010, Art. no. 163106.
[47] C. Zhao *et al.*, "An enhanced surface passivation effect in InGaN/GaN disk-in-nanowire light emitting diodes for mitigating Shockley-Read-Hall recombination.," *Nanoscale*, vol. 7, no. 40, pp. 16658–16665, 2015.
[48] H. P. T. Nguyen *et al.*, "Breaking the carrier injection bottleneck of phosphor-free nanowire white light-emitting diodes," *Nano Lett.*, vol. 13, no. 11, pp. 5437–5442, 2013.